

Gaussian beam evolution in inhomogeneous nonlinear media with absorption

PAWEŁ BERCYŃSKI

Institute of Physics, West Pomeranian University of Technology, 70-310 Szczecin, Poland

The method of complex geometrical optics (CGO) is presented, which describes Gaussian beam (GB) diffraction and self-focusing along a curvilinear trajectory in inhomogeneous and nonlinear saturable media. CGO method reduces the problem of Gaussian beam propagation in inhomogeneous and nonlinear media to solving ordinary differential equations for the complex curvature of the wave front and for GB amplitude, which can be readily solved both analytically and numerically. As a result, CGO radically simplifies the description of Gaussian beam diffraction and self-focusing effects as compared to the other methods of nonlinear optics such as: variational method approach, method of moments and beam propagation method. The power of CGO method is presented on the example of the evolution of beam cross-section and wave front cross-section along a curvilinear central ray with torsion in weakly absorptive and nonlinear saturable graded-index fibre, where the effect of initial beam ellipticity is included into our description.

Keywords: complex geometrical optics, Gaussian beam diffraction and self-focusing, nonlinear saturable media.

1. Introduction

In traditional understanding, geometrical optics is a method assigned to describe trajectories of the rays, along which the phase and amplitude of a wave field can be calculated in diffractionless approximation [1, 2]. Complex generalization of the classical geometrical optics theory allows one to include diffraction processes into the scope of consideration, which characterize wave rather than geometrical features of wave beams (by diffraction we imply here diffraction spreading of the wave beam, which is the consequence that Gaussian beam (GB) has a nature of inhomogeneous wave [3]). Although the first attempts to introduce complex rays and complex incident angles were made before the second world war, the real understanding of complex geometrical optics potential begins with publication [4], which contains the consistent definition of a complex ray. Actually there are two equivalent forms of the complex geometrical optics (CGO): the ray-based form, which deals with complex rays, *i.e.*, trajectories in complex space [2, 5–8], and the eikonal-based form, which uses

complex eikonal instead of complex rays [2, 5, 7]. The ability of CGO method to describe diffraction of GB on the basis of complex Hamilton ray equations was demonstrated many years ago in the framework of the ray-based approach. The development of numerical methods in the framework of the ray-based CGO in recent years allowed to describe GB diffraction in inhomogeneous media: GB focusing by localized inhomogeneities [9, 10], reflection from a linear-profile layer [11] as well as other problems. The passage of paraxial rays through optical structures was studied also by KOGELNIK and LI who introduced into their description a very convenient ray-transfer-matrix [12]. KOGELNIK's and LI's way of transformation is named nowadays as *ABCD* matrix method [13]. The eikonal-based CGO, which deals with complex eikonal and complex amplitude was essentially influenced by quasi-optics, which is based on parabolic wave equation (PWE) [13]. For the case of the spatially narrow wave beam concentrated in the vicinity of the central ray, the parabolic equation reduces to the truncated (parabolic) wave equation [14, 15], which preserves only quadratic terms in small deviation from the central ray. The truncated (parabolic) wave equation lets one describe electromagnetic GB evolution in optically smoothly inhomogeneous media [15]. The reduction of GB diffraction description to solving the truncated (parabolic) wave equation is an essential and convenient simplification of a quasi-optical description but still demands to solve partial differential equations. The essential step in the development of quasi-optics was taken by KOGELNIK and LI, who analyzed laser beams by introducing the (quasi-optical) complex parameter q [12] which lets one solve the parabolic equation in a more compact way taking into account the wave nature of the beams. The obtained PWE solution enables to determine the GB parameters such as beam width, amplitude and wave front curvature. The quasi-optical approach is very convenient and commonly used in the framework of beam transmission and transformation through optical systems. However, modeling of GB evolution by means of the (quasi-optical) parameter q using *ABCD* matrix is effective for GB propagation in free space or along axial symmetry in graded-index optics (on axis beam propagation) when the A , B , C , and D elements of the transformation matrix are known. Thus, the problem of GB evolution along curvilinear trajectories demands to solve the parabolic equation in a standard way which is complicated for even for inhomogeneous media [15]. In our opinion, the eikonal-based form of the paraxial CGO seems to be more powerful and simpler tool of the wave theory as compared with quasi-optics based on the parabolic equation and even with the CGO ray-based version based on Hamilton equations. It reduces the diffraction description to solving ordinary differential equations of first order. Recently, the eikonal-based CGO method has been applied to describe GB evolution in inhomogeneous media [16, 17] and nonlinear media of Kerr type [18], including graded-index [19] and nonlinear fibres [20]. It is shown in [19] that eikonal-based CGO approach demonstrates high ability to describe GB evolution in graded-index optical fibres reducing hundred times the time of numerical calculations at comparable accuracy with Crank–Nicolson scheme in beam propagation method (BPM). The present paper is organized as follows. Section 2 presents the Hamilton ray equation for a beam central ray and the ordinary Riccati-type equation

for complex wave front curvature. A corresponding transport equation for GB complex amplitude is solved in paraxial approximation and the equation for energy flux evolution is derived in Section 3. Section 4 presents numerical solutions describing a non-trivial problem of GB diffraction and self-focusing along the helical ray in a nonlinear graded-index fibre, where the evolution of GB intensity and cross-section of the beam wave-front are discussed here. Moreover, Section 4 generalizes the results of the papers [21–27] for GB evolution along a curvilinear trajectory.

2. The ray equation for a beam central ray and the Riccati equation for complex curvature

Let us consider the propagation of a monochromatic scalar Gaussian beam (see [17]) in a smoothly inhomogeneous isotropic and nonlinear saturable medium with a permittivity profile of the form

$$\varepsilon = \text{Re}(\varepsilon) + i\text{Im}(\varepsilon) = \varepsilon_R + i\varepsilon_I \tag{1}$$

where

$$\varepsilon_R = \varepsilon_{\text{LIN}}(\mathbf{r}) + \varepsilon_{\text{NL}}g[I(\mathbf{r})] \tag{2a}$$

$$\varepsilon_I = \varepsilon_1(\mathbf{r}) \tag{2b}$$

For a permittivity profile in Eq. (1) the Hamilton ray-equation written for the parameter τ can be presented in the form of a second order differential equation in a more comfortable Newtonian form

$$\frac{d^2\mathbf{r}}{d\tau^2} = \frac{1}{2} \left[\nabla\varepsilon_{\text{LIN}}(\mathbf{r}) + i\nabla\varepsilon_1(\mathbf{r}) \right] + \frac{\varepsilon_{\text{NL}}}{2} \nabla g[I(\mathbf{r})] \tag{3}$$

The nonlinear term can be neglected in Eq. (3) due to symmetry of GB with respect to the central ray. This means that the central ray of symmetric GB is not subjected to nonlinear refraction caused by a nonlinear part of relative permittivity. Therefore, the trajectory of the central ray in inhomogeneous nonlinear saturable media coincides with the central ray in the linear inhomogeneous medium with permittivity $\varepsilon(\mathbf{r}) = \varepsilon_R(\mathbf{r}) + i\varepsilon_I(\mathbf{r})$. This fact is quite helpful for an optical analysis of Gaussian beam propagation in the inhomogeneous media with saturable nonlinearities. CGO method deals with a tensor Riccati-type equation for complex curvature $B_{ij}(\tau)$ in the form

$$\frac{dB_{ij}}{d\tau} + B_{ik}B_{kj} = \beta_{ij} + \gamma_{ij} \tag{4}$$

The above Riccati-type equation for the parameter $B_{ij}(\tau)$ is a system of three equations:

$$\frac{dB_{11}}{d\tau} + (B_{11}^2 + B_{12}^2) = \beta_{11} + \gamma_{11} \tag{5a}$$

$$\frac{dB_{12}}{d\tau} + B_{12}(B_{11} + B_{22}) = \beta_{12} + \gamma_{12} \quad (5b)$$

$$\frac{dB_{22}}{d\tau} + (B_{22}^2 + B_{12}^2) = \beta_{22} + \gamma_{22} \quad (5c)$$

The terms quadratic in B_{ij} in Eq. (4) are responsible for diffraction in homogeneous medium. The right-hand side terms β_{ij} in Eq. (4) describes the influence of linear refraction on GB diffraction, whereas quantities γ_{ij} take into account the influence of self-focusing of GB. These parameters have the forms

$$\beta_{ij}(\tau) = \left[\frac{1}{2} \frac{\partial^2 \varepsilon(\mathbf{r})}{\partial \xi_i \partial \xi_j} - \frac{3}{4\varepsilon(\mathbf{r})} \frac{\partial \varepsilon(\mathbf{r})}{\partial \xi_i} \frac{\partial \varepsilon(\mathbf{r})}{\partial \xi_j} \right]_{\mathbf{r}=\mathbf{r}_c} \quad (6)$$

$$\gamma_{ij}(\tau) = \left[\frac{\varepsilon_{NL}}{2} \frac{\partial g}{\partial I} \frac{\partial^2 I(\mathbf{r})}{\partial \xi_i \partial \xi_j} \right]_{\mathbf{r}=\mathbf{r}_c} \quad (7)$$

Equations (4) are the basic equations for description of GB diffraction in smoothly inhomogeneous and nonlinear media. It is worth noting that Eqs. (4) are ordinary differential equations, which are very useful for the analysis and numerical simulations. Thus, the method under consideration has a great advantage over the parabolic equation approximation [13–15]. The complex Eqs. (5) can be presented as a system of six real equations for quantities $R_{ij} \equiv \text{Re}(B_{ij})$ and $I_{ij} \equiv \text{Im}(B_{ij})$:

$$\frac{dR_{11}}{d\tau} + R_{11}^2 + R_{12}^2 - I_{11}^2 - I_{12}^2 = \beta_{11} + \gamma_{11} \quad (8a)$$

$$\frac{dR_{12}}{d\tau} + R_{12}(R_{11} + R_{22}) - I_{12}(I_{11} + I_{22}) = \beta_{12} + \gamma_{12} \quad (8b)$$

$$\frac{dR_{22}}{d\tau} + R_{22}^2 + R_{12}^2 - I_{22}^2 - I_{12}^2 = \beta_{22} + \gamma_{22} \quad (8c)$$

$$\frac{dI_{11}}{d\tau} + 2R_{11}I_{11} + 2R_{12}I_{12} = 0 \quad (8d)$$

$$\frac{dI_{12}}{d\tau} + R_{12}(I_{11} + I_{22}) + I_{12}(R_{11} + R_{22}) = 0 \quad (8e)$$

$$\frac{dI_{22}}{d\tau} + 2R_{22}I_{22} + 2R_{12}I_{12} = 0 \quad (8f)$$

If we denote the eigenvalues of tensors $R_{ij}(\tau)$ and $I_{ij}(\tau)$ as $R_i(\tau)$ and $I_i(\tau)$, principal curvatures of the wave front as κ_i and the beam principal widths as w_i , then we obtain that:

$$R_i = \sqrt{\varepsilon_c} \kappa_i, \quad I_i = \frac{1}{k_0 w_i^2} \tag{9}$$

The principal beam widths and principle curvatures of the wave front are equal to:

$$w_{1,2}^2 = \frac{4}{k_0 \left[I_{11} + I_{22} \pm \sqrt{(I_{11} - I_{22})^2 + 4I_{12}^2} \right]} \tag{10a}$$

$$\kappa_{1,2} = \frac{R_{11} + R_{22} \pm \sqrt{(R_{11} - R_{22})^2 + 4R_{12}^2}}{2\sqrt{\varepsilon_c}} \tag{10b}$$

3. Equation for complex amplitude and flux evolution in weakly absorptive media

In the ray-centered coordinates (τ, ξ_1, ξ_2) the transport equation [2] takes the form

$$2(\nabla A \cdot \nabla \psi) + A \nabla \psi + k_0 \varepsilon_1 A = 0 \tag{11}$$

By using paraxial approximation and introducing new amplitude $\tilde{A} = \varepsilon_c^{1/4} A$, the above equation can be reduced to the following form

$$\frac{d\tilde{A}^2}{d\tau} + \text{Tr} B_{ij} \tilde{A}^2 + k_0 \varepsilon_1(\mathbf{r}) \tilde{A}^2 = 0 \tag{12}$$

where $\text{Tr} B_{ij} \equiv B_{ii} = B_{11} + B_{22}$. It admits an explicit solution

$$\tilde{A}^2 = \tilde{A}_0^2 \exp\left(-\int \text{Tr} B_{ij} d\tau\right) \exp\left(-k_0 \int \varepsilon_1(\mathbf{r}) d\tau\right) \tag{13}$$

where $\tilde{A}_0 = \tilde{A}(0)$ is the initial amplitude of the beam. The above solution leads to the equation which describes energy flux evolution in nonlinear medium with absorption and has the form

$$w_1 w_2 |\tilde{A}|^2 = w_1(0) w_2(0) |\tilde{A}_0|^2 \exp\left(-k_0 \int \varepsilon_1(\mathbf{r}) d\tau\right) \tag{14}$$

4. GB diffraction and self-focusing along a helical ray in a nonlinear graded-index fibre

Let us consider axially symmetrical focusing medium in cylindrical coordinates (r, φ, z) with dielectric permittivity

$$\varepsilon = \varepsilon_0 + i\varepsilon_1 - \frac{r^2}{L^2} + \frac{\varepsilon_{NL} I}{1 + \varepsilon_{NL} I / \varepsilon_s} \tag{15}$$

where ε_s denotes saturating permittivity and $r = \sqrt{x^2 + y^2}$ is the distance from the axis z (radius in cylindrical symmetry), $I = cuu^*/4\pi$ is beam intensity (see [17]), $L \sim \varepsilon_{\text{LIN}}/|\nabla\varepsilon_{\text{LIN}}|$ is the characteristic inhomogeneity scale of the fibre which is related with the fibre core radius r_c by the relation $L = r_c/\delta$, where δ is the difference of the constant refractive indexes between the core and the cladding and ε_0 is permittivity along the symmetry axis. We assume here that the imaginary part of complex permittivity does not change significantly in the range of either the fibre inhomogeneity scale L or the diffraction distance of the beam $L_D = k_0 w_0^2$, thus $\varepsilon_1/|\nabla\varepsilon_1| \gg L$, $\varepsilon_1/|\nabla\varepsilon_1| \gg L_D$, and as a result the imaginary part ε_1 of complex permittivity ε in Eq. (15) can be approximately admitted to be constant ($\varepsilon_1 = \text{const}$). The permittivity profile in Eq. (15) models inhomogeneous and nonlinear optical fibres [21], which for low intensities $I \rightarrow 0$ has a Kerr type profile

$$\varepsilon = \varepsilon_0 + i\varepsilon_1 - \frac{r^2}{L^2} + \varepsilon_{\text{NL}}I \quad (16)$$

and which saturates for $I \rightarrow \infty$, resulting in

$$\varepsilon = \varepsilon_0 + i\varepsilon_1 - \frac{r^2}{L^2} + \varepsilon_s \quad (17)$$

The GB incidence on fibre's core is defined by a unit tangent vector \mathbf{I} with respect to the central ray that possesses a component in the azimuthal direction \mathbf{I}_φ and along the fibre symmetry axis \mathbf{I}_z . As shown in Eq. (3) with conclusions below we obtain that

$$\frac{\varepsilon_{\text{NL}}}{2} \nabla g [I(\mathbf{r})] = 0 \quad \text{and} \quad \nabla \varepsilon_1 = 0 \quad (18)$$

One can notice that the nonlinearity and the effect of absorption modeled by constant imaginary part of complex electric permittivity do not influence the central ray evolution but influence only the amplitude, the wave front curvature and the beam width. As a result, the GB propagates along a helical ray like in linear inhomogeneous medium with a constant radius r_c , which equals [1, 2]:

$$r_c = -l_\varphi^2 \frac{2\varepsilon}{\varepsilon'} \Big|_{r=r_c} \quad (19)$$

where l_φ is the axial component of a unit tangent vector \mathbf{I} and prime stand for the derivatives with respect to r . Substituting Eq. (15) into Eq. (19) and taking into account Eq. (18), we have the radius of the central ray which is equal to

$$r_c = \frac{l_\varphi \sqrt{\varepsilon_0}}{\sqrt{1 + l_\varphi^2}} L \quad (20)$$

and the torsion of this helical ray is equal to:

$$\chi = \frac{l_z l_\varphi}{r_c} = \frac{\sqrt{1-l_\varphi^4}}{\sqrt{\varepsilon_0} L} = \text{const} \tag{21}$$

where $l_z = \sqrt{1-l_\varphi^2}$, since $l_r = 0$. The normal and binormal to the ray are connected to the units vectors of the cylindrical coordinates as

$$\mathbf{n} \equiv -\mathbf{e}_r, \quad \mathbf{b} \equiv -(l_z \mathbf{e}_\varphi - l_\varphi \mathbf{e}_z) \tag{22}$$

We introduce the coordinate system corresponding to the parallel transport (see [17]):

$$\mathbf{e}_1 = -\mathbf{e}_r \cos(\theta) - (l_z \mathbf{e}_\varphi - l_\varphi \mathbf{e}_z) \sin(\theta) \tag{23a}$$

$$\mathbf{e}_2 = -(l_z \mathbf{e}_\varphi - l_\varphi \mathbf{e}_z) \cos(\theta) + \mathbf{e}_r \sin(\theta) \tag{23b}$$

where

$$\theta = -\frac{\sqrt{1-l_\varphi^2}}{L} \tau \tag{24}$$

is the rotation angle of the normal \mathbf{n} around the ray. To solve Eqs. (4), it is necessary to determine functions $\beta_{ij}(\tau)$ and $\gamma_{ij}(\tau)$ in a coordinate system (τ, ξ_1, ξ_2) with unit vectors in Eqs. (23). Taking into account that $\partial/\partial \xi_i = (\mathbf{e}_i \nabla)$ and that for an axially inhomogeneous medium $\nabla = \mathbf{e}_r d/dr$, one can rewrite Eq. (6) as

$$\beta_{ij} = (\mathbf{e}_i \mathbf{e}_r)(\mathbf{e}_j \mathbf{e}_r) \left[\frac{\varepsilon''}{2} - \frac{3\varepsilon'^2}{4\varepsilon} \right] \tag{25}$$

where the prime stands for the derivative with respect to r . In view of Eqs. (22) and (23) these expressions take the form

$$\beta_{11} = -\frac{1+3l_\varphi^2}{L^2} \cos^2(\theta) \tag{26a}$$

$$\beta_{12} = \beta_{21} = \frac{1+3l_\varphi^2}{L^2} \sin(\theta) \cos(\theta) \tag{26b}$$

$$\beta_{22} = -\frac{1+3l_\varphi^2}{L^2} \sin^2(\theta) \tag{26c}$$

If we include into our description the saturating nonlinearity of the fibre, the parameters γ_{ij} in Eq. (7), taking into account Eqs. (14) and (18), take the form:

$$\gamma_{11} = \frac{-k_0^2 \varepsilon_{NL} I_0 w_{10} w_{20} I_{11} \sqrt{I_{11} I_{22} - I_{12}^2} \exp(-k_0 \varepsilon_1 \tau)}{\left[1 + \varepsilon_{NL} I_0 w_{10} w_{20} \sqrt{I_{11} I_{22} - I_{12}^2} \exp(-k_0 \varepsilon_1 \tau) / \varepsilon_s \right]^2} \quad (27a)$$

$$\gamma_{12} = \frac{-k_0^2 \varepsilon_{NL} I_0 w_{10} w_{20} I_{12} \sqrt{I_{11} I_{22} - I_{12}^2} \exp(-k_0 \varepsilon_1 \tau)}{\left[1 + \varepsilon_{NL} I_0 w_{10} w_{20} \sqrt{I_{11} I_{22} - I_{12}^2} \exp(-k_0 \varepsilon_1 \tau) / \varepsilon_s \right]^2} \quad (27b)$$

$$\gamma_{22} = \frac{-k_0^2 \varepsilon_{NL} I_0 w_{10} w_{20} I_{22} \sqrt{I_{11} I_{22} - I_{12}^2} \exp(-k_0 \varepsilon_1 \tau)}{\left[1 + \varepsilon_{NL} I_0 w_{10} w_{20} \sqrt{I_{11} I_{22} - I_{12}^2} \exp(-k_0 \varepsilon_1 \tau) / \varepsilon_s \right]^2} \quad (27c)$$

where $w_{10} = w_1(0)$, $w_{20} = w_2(0)$ and I_0 is the initial intensity of GB propagating in a nonlinear inhomogeneous fibre. For the incident angle φ_0 , which is the angle between vectors \mathbf{l}_z and \mathbf{l} in $\tau = 0$, we obtain that $l_z = \cos(\varphi_0)$ and $l_\varphi = \sin(\varphi_0)$. The Equations (8a)–(8f) together with Eqs. (27a)–(27c) are solved numerically for the following parameters: $\varepsilon_0 = 2$, $L = 200\lambda$, $\varphi_0 = 45^\circ$ ($l_\varphi = 1/\sqrt{2}$) and in particular cases for different values of $\varepsilon_{NL} I_0 = \varepsilon_{NL} I(\tau = 0)$, $\varepsilon_1 = \varepsilon_1(\tau = 0) = \text{const}$, $w_{20}/w_{10} = w_2(\tau = 0)/w_1(\tau = 0)$, $\kappa_{10} = \kappa_1(\tau = 0)$ and $\kappa_{20} = \kappa_2(\tau = 0)$ presented below in Figs. 1–3. CGO method presented in this paper enables also to perform explicitly the evolution of the beam cross-section, which is determined by the equation $k_0 I_{ij}(\tau) \xi_i \xi_j = 1$ and the cross-section

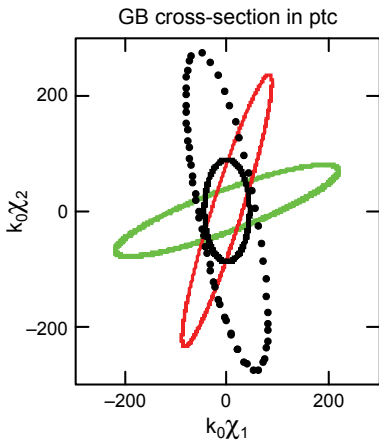


Fig. 1. Evolution of GB (with initial ellipticity $w_{20} = 2w_{10}$) cross-section in parallel transport coordinates (ptc) (ξ_1, ξ_2) for GB propagating along a helical ray with parameters $\varepsilon_{NL} I_0 = 10^{-6}$, $\varepsilon_1 = 10^{-4}$. The images of GB cross-section are shown for the values of τ : black continuous trace ($\tau = 0$), green trace ($\tau = L_D$), red trace ($\tau = 3L_D$) and dotted black trace ($\tau = 5L_D$), where $w_{10} = 10^{-5}$ m, $\kappa_{10} = \kappa_{20} = 0$ and $L_D = k_0 w_{10}^2 = 6.3 \times 10^{-4}$ m.

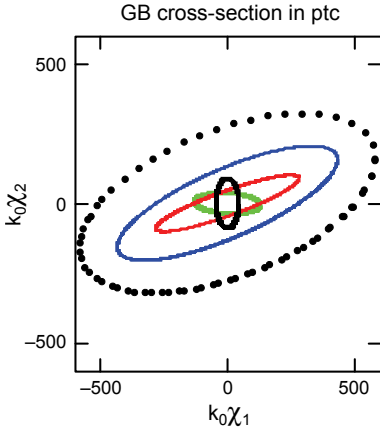


Fig. 2. Evolution of GB (with initial ellipticity $w_{20} = 2w_{10}$) cross-section in parallel transport coordinates (ptc) (ξ_1, ξ_2) for GB propagating along a helical ray with parameters $\varepsilon_{NL}I_0 = 10^{-2}$, $\varepsilon_1 = 10^{-3}$. The images of GB cross-section are shown for the values of τ : black continuous trace ($\tau = 0$), green trace ($\tau = L_D$), red trace ($\tau = 2L_D$), blue trace ($\tau = 3L_D$) and dotted black trace ($\tau = 4L_D$), where $w_{10} = 10^{-5}$ m, $\kappa_{10} = \kappa_{20} = 0$ and $L_D = k_0 w_{10}^2 = 6.3 \times 10^{-4}$ m.

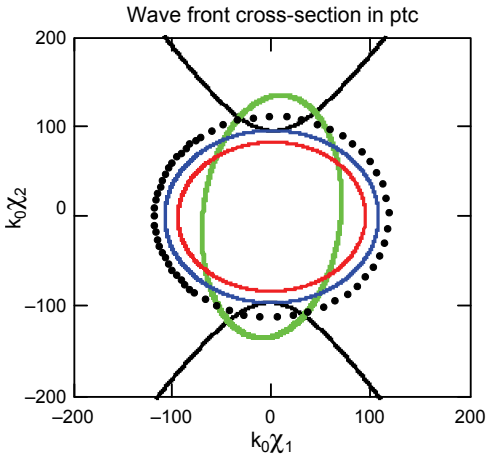


Fig. 3. Evolution of GB wave front cross-section in parallel transport coordinates (ptc) (ξ_1, ξ_2) for GB propagating along a helical ray with parameters $\varepsilon_{NL}I_0 = 10^{-2}$, $\varepsilon_1 = 10^{-3}$. The images of GB cross-section are shown for the values of τ : black continuous trace ($\tau = L_D$), green trace ($\tau = 2L_D$), red trace ($\tau = 3L_D$), blue trace ($\tau = 4L_D$) and dotted black trace ($\tau = 5L_D$), where $w_{10} = 10^{-5}$ m, $\kappa_{10} = \kappa_{20} = 0$, $w_{20} = 2w_{10}$ and $L_D = k_0 w_{10}^2 = 6.3 \times 10^{-4}$ m.

of the GB wave front, where $k_0 R_{ij}(\tau) \xi_i \xi_j = 1$ in parallel transport coordinates (ξ_1, ξ_2) . In Figures 1 and 2 we show the evolution of the beam cross-section and in Fig. 3 the evolution of GB wave front cross-section in parallel transport coordinates (ξ_1, ξ_2) .

We notice that non-zero torsion of the central ray causes non-trivial parallel transport, Eqs. (23), and leads to the entanglement of equations, because the inhomogeneity influence, *i.e.*, the parameter β_{ij} in the right-hand sides of Eqs. (4), is linked up

to normal–binormal coordinate system ($\nabla\mathcal{E}$ lies in the (\mathbf{l}, \mathbf{n}) plane, see [1, 2], whereas the second parameter γ_{ij} depends on the parameters of GB cross-section $I_{ij}(\tau)$ from the left-hand side of Eq. (14) including also the parameter $\sqrt{I_{11}I_{22} - I_{12}^2}$, which is related with the surface of GB spot by the relation $1/w_1w_2$. In Figure 1 we present the evolution of GB cross-section with initial ellipticity $w_{20} = 2w_{10}$ in parallel transport coordinates (ξ_1, ξ_2) for GB propagating along a helical ray in a nonlinear graded-index fibre with absorption, where $\varepsilon_{\text{NL}}I_0 = 10^{-6}$ and $\varepsilon_1 = 10^{-4}$. One can see that the large axis of beam's cross-section rotates in (ξ_1, ξ_2) coordinates in negative (anti-clockwise) direction with angular velocity, that approximately equals $d\theta/d\tau = -\sqrt{\varepsilon_c} \chi_c$, where

$$\begin{aligned} \varepsilon_c &= \varepsilon_0 - \frac{r_c^2}{L^2} + \frac{\varepsilon_{\text{NL}}I}{1 + \varepsilon_{\text{NL}}I/\varepsilon_s} = \\ &= \varepsilon_0 - \frac{r_c^2}{L^2} - \frac{\varepsilon_{\text{NL}}I_0w_{10}w_{20}\sqrt{\varepsilon_c(0)} \varepsilon_s\sqrt{I_{11}I_{22} - I_{12}^2} \exp(-k_0\varepsilon_1\tau)}{\sqrt{\varepsilon_c} \varepsilon_s + \varepsilon_{\text{NL}}I_0w_{10}w_{20}\sqrt{I_{11}I_{22} - I_{12}^2} \exp(-k_0\varepsilon_1\tau)} \end{aligned} \quad (28)$$

One can notice using Eq. (28) that for the distance of a few diffraction distances, taking into account also the parameters in Figs. 1–3, we obtain in good approximation that

$$\begin{aligned} \varepsilon_c &= \varepsilon_0 - \frac{r_c^2}{L^2} - \frac{\varepsilon_{\text{NL}}I_0w_{10}w_{20}\sqrt{\varepsilon_c(0)} \varepsilon_s\sqrt{I_{11}I_{22} - I_{12}^2} \exp(-k_0\varepsilon_1\tau)}{\sqrt{\varepsilon_c} \varepsilon_s + \varepsilon_{\text{NL}}I_0w_{10}w_{20}\sqrt{I_{11}I_{22} - I_{12}^2} \exp(-k_0\varepsilon_1\tau)} \cong \\ &\cong \varepsilon_0 - \frac{r_c^2}{L^2} = \frac{4}{3} \end{aligned} \quad (29)$$

In Figure 2 we present the evolution of GB cross-section with initial ellipticity $w_{20} = 2w_{10}$ for parameters $\varepsilon_{\text{NL}}I_0 = 10^{-2}$, $\varepsilon_1 = 10^{-3}$. One can notice that for the distance of two and a half diffraction distances, the large axis of beam's cross-section rotates in (ξ_1, ξ_2) coordinates in anti-clockwise direction and after achieving the distance of $\tau_D = 2.5L_D$, the GB cross-section conserves its orientation being stretched to ξ_1 direction. However, the cross-section ellipse is not exactly oriented along ξ_1 axes, as it is seen in Fig. 2, but it is slightly inclined in anti-clockwise direction. The inclined orientation of the cross-section ellipse reflects some sort of balance between the dominated parallel transport and the tendency of inhomogeneous symmetry and GB self-focusing to rotate the beam spot in anti-clockwise direction. We notice that GB cross-section first of all experiences a diffraction widening effect resulting in GB principle width along a large axis increasing fast similar to Fig. 1. Moreover, due to stronger absorption effect which limits self-focusing of the beam, the principle width along a minor axis increases faster as compared with Fig. 1. From our numerical calculations

we observe that GB cross-section conserves its orientation through next few diffraction distances after which CGO method becomes inapplicable. Let us recall that CGO boundary applicability demands that principle GB widths should be small as compared with characteristic fibre inhomogeneity scale $\mu_{\text{REF}} = w_0/L \ll 1$. Thus the fast increase in GB cross-section surface makes impossible further examination of the evolution of GB cross-section, which becomes comparable with the radius of the core. In Figure 3 we present the evolution of GB wave front cross-section for GB propagating along a helical ray with parameters $\varepsilon_{\text{NL}}I_0 = 10^{-2}$, $\varepsilon_1 = 10^{-3}$. We notice that initially a hyperbolic wave front transforms into an elliptical one at the distance of two diffraction distances. Next large axis of an elliptical wave front cross-section rotates in clockwise direction from ξ_2 to ξ_1 axis. After the distance of four diffraction distances, the wave front cross-section becomes attached to ξ_1 axis.

5. Conclusions

The paper applies the method of complex geometrical optics (CGO) to the analysis of the GB evolution in smoothly inhomogeneous and nonlinear saturable media. The CGO method reduces the diffraction problem for the Gaussian beam to a solution of ordinary differential equations, describing the behaviour of the amplitude, the beam width and the curvature of the wave front. Following analogously like in papers [21–24], we model the light propagation in nonlinear fibres by Gaussian beam, which is self-sustained solution within the CGO method. CGO method readily provides a solution for an inhomogeneous nonlinear saturable fibre in a simpler way than the standard methods of nonlinear optics such as the variation method approach, method of moments and beam propagation method. Besides simplicity and affectivity, the CGO method supplies a number of new results. Firstly, it is shown that the central ray of Gaussian beam is not affected by the nonlinear refraction. As a result, the beam trajectory propagates analogously like in linear inhomogeneous medium but nonlinearity influences only GB parameters such as amplitude, width and wave front curvature. This fact enables one to perform simply and effectively simulations of light beam diffraction and self-focusing for the case of GB incidence at an angle on the surface of the core of nonlinear inhomogeneous fibres. Secondly, it is shown in the paper how weak absorption influences GB evolution along a curvilinear trajectory in a nonlinear saturable fibre. Thirdly, we show explicitly the evolution of beam cross-section and wave front cross-section for GB propagating along a helical ray in a nonlinear inhomogeneous fibre with absorption. This way CGO method demonstrates high ability in sophisticated applications of nonlinear graded-index optics in both experimental and theoretical problems.

References

- [1] KRAVTSOV YU.A., ORLOV YU.I., *Geometrical Optics of Inhomogeneous Medium*, Springer-Verlag, Berlin, 1990.

- [2] KRAVTSOV YU. A., ZHU N.Y., *Theory of Diffraction: Heuristic Approaches*, Alpha Science International, 2009.
- [3] DESCHAMPS G.A., *Gaussian beam as a bundle of complex rays*, Electronics Letters **7**(23), 1971, pp. 684–685.
- [4] KELLER J.B., *A geometrical theory of diffraction*, [In] *Calculus of Variations and its Applications, Proceedings of Symposia in Applied Mathematics*, Vol. 8, McGraw-Hill, New York, 1958, pp. 27–52.
- [5] KRAVTSOV YU.A., FORBES G.W., ASATRYAN A.A., *Theory and applications of complex rays*, [In] *Progress in Optics*, [Ed.] E. Wolf, Vol. 39, Elsevier, Amsterdam, 1999, pp. 3–62.
- [6] CHAPMAN S.J., LAWRY J.M.H., OCKENDON J.R., TEW R.H., *On the theory of complex rays*, SIAM Review **41**(3), 1999, pp. 417–509.
- [7] KRAVTSOV YU.A., *Complex rays and complex caustics*, Radiophysics and Quantum Electronics **10**(9–10), 1967, pp. 719–730.
- [8] KELLER J.B., STREIFER W., *Complex rays with application to Gaussian beams*, Journal of the Optical Society of America **61**(1), 1971, pp. 40–43.
- [9] EGORCHENKOV R.A., KRAVTSOV YU.A., *Numerical implementation of complex geometrical optics*, Radiophysics and Quantum Electronics **43**(7), 2000, pp. 569–575.
- [10] EGORCHENKOV R.A., KRAVTSOV YU.A., *Complex ray-tracing algorithms with application to optical problems*, Journal of the Optical Society of America A **18**(3), 2001, pp. 650–656.
- [11] EGORCHENKOV R.A., *Wave fields in inhomogeneous media numerically calculated on the basis of complex geometrical optics*, Physics of Vibrations **8**, 2000, pp. 122–127.
- [12] KOGELNIK H., LI T., *Laser beams and resonators*, Applied Optics **5**(10), 1966, pp. 1550–1567.
- [13] ARNAUD J.A., *Beam and Fiber Optics*, Academic Press, San Diego, 1976.
- [14] VLASOV S.N., TALANOV V.I., *The parabolic equation in the theory of wave propagation*, Radiophysics and Quantum Electronics **38**(1–2), 1995, pp. 1–12.
- [15] PERMITIN G.V., SMIRNOV A.I., *Quasioptics of smoothly inhomogeneous isotropic media*, Journal of Experimental and Theoretical Physics **82**(3), 1996, pp. 395–402.
- [16] BERCZYNSKI P., KRAVTSOV YU.A., *Theory for Gaussian beam diffraction in 2D inhomogeneous medium, based on the eikonal form of complex geometrical optics*, Physics Letters A **331**(3–4), 2004, pp. 265–268.
- [17] BERCZYNSKI P., BLOKH K.YU., KRAVTSOV YU.A., STATECZNY A., *Diffraction of a Gaussian beam in a three-dimensional smoothly inhomogeneous medium: an eikonal-based complex geometrical-optics approach*, Journal of the Optical Society of America A **23**(6), 2006, pp. 1442–1451.
- [18] BERCZYNSKI P., KRAVTSOV YU.A., SUKHORUKOV A.P., *Complex geometrical optics of Kerr type nonlinear media*, Physica D: Nonlinear Phenomena **239**(5), 2010, pp. 241–247.
- [19] BERCZYNSKI P., KRAVTSOV YU.A., ZEGLINSKI G., *Gaussian beam diffraction in inhomogeneous media of cylindrical symmetry*, Optica Applicata **40**(3), 2010, pp. 705–718.
- [20] BERCZYNSKI P., *Complex geometrical optics of nonlinear inhomogeneous fibres*, Journal of Optics **13**(3), 2011, article 035707.
- [21] BISWAS A., *Theory of non-Kerr law solitons*, Applied Mathematics and Computation **153**(2), 2004, pp. 369–385.
- [22] YIJIAN CHEN, *Self-trapped light in saturable nonlinear media*, Optics Letters **16**(1), 1991, pp. 4–6.
- [23] GREEN P.D., MILOVIC D.M., LOTT D.A., BISWAS A., *Dynamics of Gaussian optical solitons by collective variables method*, Applied Mathematics and Information Sciences **2**(3), 2008, pp. 259–273.
- [24] LOTT D.A., HENRIQUEZ A., STURDEVANT B.J.M., BISWAS A., *Optical soliton-like structures resulting from the nonlinear Schrödinger's equation with saturable law nonlinearity*, Applied Mathematics and Information Sciences **5**(1), 2011, pp. 1–16.
- [25] BISWAS A., MILOVIC D., MAJID F., KOHL R., *Optical soliton cooling in saturable law media*, Journal of Electromagnetic Waves and Applications **22**(13), 2008, pp. 1735–1746.

- [26] GIRGIS L., MILOVIC D., KONAR S., YILDIRIM A., JAFARI H., BISWAS A., *Optical gausssons in birefringent fibers and DWDM systems with intermodal dispersion*, Romanian Reports in Physics **64**(3), 2012, pp. 663–671.
- [27] GIRGIS L., MILOVIC D., HAYAT T., ALDOSSARY O.M., BISWAS A., *Optical soliton perturbation with log law nonlinearity*, Optica Applicata **42**(3), 2012, pp. 447–454.

Received January 21, 2013